Available online at www.sciencedirect.com

ScienceDirect

Procedia Manufacturing 26 (2018) 424–433

Procedia MANUFACTURING

www.elsevier.com/locate/procedia

46th SME North American Manufacturing Research Conference, NAMRC 46, Texas, USA

Performance analysis of Nano Engineered Diamond coated tools for machining of AA2124/SiC_p composite material

K.Ramasubramanian[a,b] , N.Arunachalam[a]*, M.S.Ramachandra Rao[b]

[a]*Department of Mechanical Engineering, Indian Institute of Technology Madras, Chennai 600036, India*
[b]*Nano Functional Materials Technology Centre, Indian Institute of Technology Madras, Chennai 600036, India*
[c]*Department of Physics, Indian Institute of Technology Madras, Chennai 600036, India*

* Corresponding author. Tel.: +91 044 22574722; fax: +0-000-000-0000 .
E-mail address: chalam@iitm.ac.in

Abstract

Aluminum based metal matrix composites (Al-SiC) are widely used in automotive and aerospace industries due to its high strength to weight ratio, high wear resistance, and higher thermal conductivity. Though it has lots of commercial applications, machining of this MMC still a challenging task due to its hard SiC reinforcement in the soft aluminum material. These two phases cause adhesive and abrasive wear on the cutting tool. Hence tooling with a property of combined hardness and toughness required to machine this material effectively. In this connection, CVD diamond on WC-Co is considered as the suitable cutting tool for the precise machining of this MMC material. Even though it is commercially available, the usage is limited due to the poor interfacial adhesion of CVD diamond on WC-Co leads to coating delamination. In this work, the boron doped diamond (BDD) and boron doped graded layer diamond coating (BMTN) on WC-Co were considered. Machining experiments were conducted on a lathe using AA2124/SiCp MMC material to evaluate the wear performance of the BMTN, BDD, MCD (Microcrystalline diamond coating) and NCD (Nanocrystalline diamond coating) coated cutting inserts. The tool wear results indicate that the BMTN outperformed in comparison with MCD and NCD coated tool inserts.

Peer-review under responsibility of the scientific committee of the 46th SME North American Manufacturing Research Conference.

Keywords: MCD; NCD; BDD; BMTN; Al-SiC MMC

2351-9789
Peer-review under responsibility of the scientific committee of the 46th SME North American Manufacturing Research Conference.
10.1016/j.promfg.2018.07.050

1. Introduction

Metal matrix composites (MMC) are widely used in automotive and aerospace industries due to its enhanced mechanical properties such as high strength-weight ratio, higher thermal conductivity, and higher stiffness compared to the monolithic aluminum alloy. In particular, aluminum-copper alloy reinforced with SiC particles (AA2124/SiCp) is used in pistons, cylinder liners, connecting rods, and brake calipers and chassis components. In addition, these materials are used in aero-engine parts and aircraft structure. Though these materials usage is widespread, still in manufacturing community this MMC is considered as a difficult to machine material. This could be due to the hard abrasive nature of SiC particles present in the soft phase of the aluminum material. Inappropriate tooling leads to surface damage of work-piece and increases the final cost of the manufactured product. In this regard, many researchers investigated the machinability of aluminum-based composites with different tooling types such as carbide tools and PCBN tools. Hung et.al [1] and Tomac et.al [2] investigated the machinability of Al-SiC by carbide tools and found that tools are subjected to rapid flank wear due to higher hardness of SiC particle in MMC which leads to abrasive wear. Ciftci et.al [3] studied machining of MMC by CBN tools and found that tools subjected to heavy fracture in both cutting edge and nose. In this connection, most literature [4, 5] [6] reported that diamond based cutting tools found to be a suitable candidate for machining of MMC effectively due to its properties of high hardness, high thermal conductivity and chemically inert with aluminum material.

Diamond-based cutting tools are classified into polycrystalline diamond tools (PCD) and CVD Diamond coated WC-Co and Diamond-like carbon (DLC) respectively. Though PCD tools perform better in machining MMC, it is highly expensive and difficult to fabricate for the complicated geometry of the cutting tools [7]. The DLC coated cutting tool is not suitable for MMC machining due to its lower hardness, because of its amorphous nature of the phase [8]. The uniform diamond growth on the complicated geometry of carbide cutting tools by the CVD diamond coating is a suitable alternative to PCD in terms of cost and its fabrication [9]. However, in conventional CVD diamond (MCD, NCD) on WC-Co, coating delaminating is a common failure due to graphitization issue by cobalt binder. Thus, many works have been done on the coating aspect to hinder the diffusion of cobalt from WC-Co.

Surface modification such as chemical etching, laser treatment and plasma treatment on carbide tools can reduce the surface cobalt to considerable level [10-12]. However, during deposition, in-situ suppression of cobalt diffusion is highly a difficult task. Thus research directed towards different interlayers such as SiC, Si_3N_4, and CrN on WC-Co before diamond deposition. Though interlayer's provided adequate adhesion, the final cost involved in the diamond coated cutting tool found to be expensive. In this context, boron doped diamond on WC-Co is a recent work in diamond-carbide adhesion improvement, where incorporation of boron in the diamond lattice can improve the interfacial adhesion through boron – cobalt interactions [13-15]. In one of our latest work [16], a study on the effect of boron doping on interfacial adhesion strength of CVD diamond coated WC-Co was carried out. The results indicate that the boron doped graded layer diamond coated tool was found to have better adhesion strength in comparison with MCD, NCD coating.

This improved adhesion in the diamond-carbide interface through boron doping expected to provide better performance during machining of AA2124/SiC material. Thus a systematic study was done by using a boron-doped diamond (BDD) and boron doped graded layer diamond coated (BDD/Transition layer/NCD) tools for machining this MMC material effectively.

Nomenclature

ϕ	Principal cutting edge angle (º)
γ^o	Orthogonal Rake angle (º)
γ_n	Normal rake angle (º)
r	Nose radius (mm)
t	Coating thickness (μm)
λ	Inclination angle (º)

2. Experimental work

2.1 Cutting tool and coating process

The cemented tungsten carbide (WC-Co) with SPUN 120308 grade was chosen as a substrate material for diamond deposition. The cutting tool angles such as major cutting edge angle, minor cutting edge angle, orthogonal rake angle and nose radius values are listed in Table.1. The schematic view of the WC-Co cutting insert (ISO code: SPUN 120308) was shown in Fig.1.

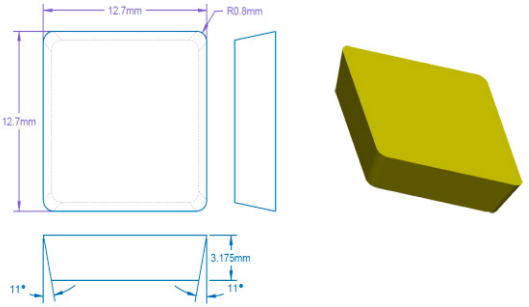

Fig.1. Schematic views of WC-Co cutting insert

Prior to diamond deposition, cobalt etching was done on WC-Co insert for all four coating variants to remove surface cobalt from 4.85% (WC-Co: weight %) to 0.19% (Cobalt etched: weight %) as shown in Fig.2. The presence of cobalt in the diamond-carbide interface negatively affects the interface adhesion.

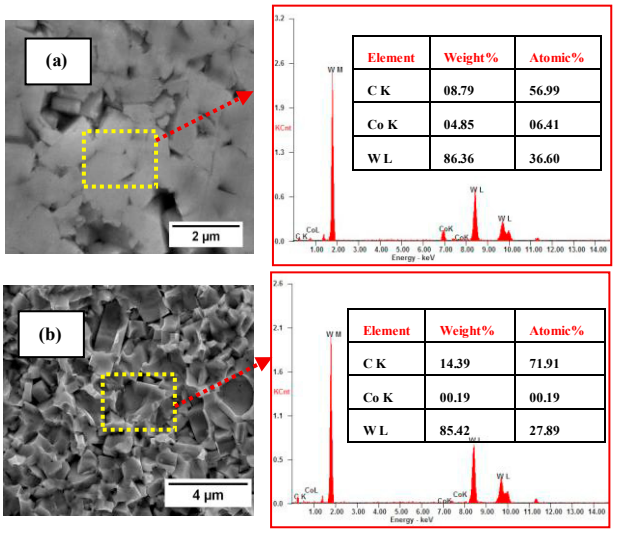

Fig.2. Surface treatment on WC-Co cutting insert
a) Untreated WC-Co insert; b) Cobalt etched WC-Co insert

Table.1. Cutting tool types and angles

S.No	Type of tool	t (µm)	ϕ_1 (°)	ϕ_2 (°)	γ^o (°)	r (mm)
1	WC-Co		75	15	5	0.8
2	MCD/ WC-Co	4-5	75	15	5	0.8
3	NCD/ WC-Co	4-5	75	15	5	0.8
4	BDD/ WC-Co	4-5	75	15	5	0.8
5	BMTN/ WC-Co	4-5	75	15	5	0.8

Diamond nucleation density will be high for carbide cutting tool, hence uniform deposition of diamond films throughout the cutting tool can be achieved. The diamond coating was fabricated using hot filament CVD reactor (HFCVD). The process parameters such as methane concentration, chamber pressure, and substrate temperature were optimized for distinct morphological variation of the diamond coating. The detailed process parameters were shown in Table.2

Table.2. Diamond deposition condition

Diamond films	Filament Temperature (°C)	Substrate Temperature (°C)	CH_4/H_2 Ratio (%)	Boron Concentration (%)
MCD	2200±20	850	2	
NCD	2200±20	850	4	
BDD	2200±20	850	2	0.22
BDD	2200±20	850	2	0.22
Transition Layer	2200±20	850	Slowly changes from BDD to NCD	
NCD	2200±20	850	4	

The four coating variants such as MCD, NCD, BDD, and BMTN were grown on WC-Co cutting tool with a uniform coating thickness of 4-5 µm as listed in Table.1 and shown in Fig.3.

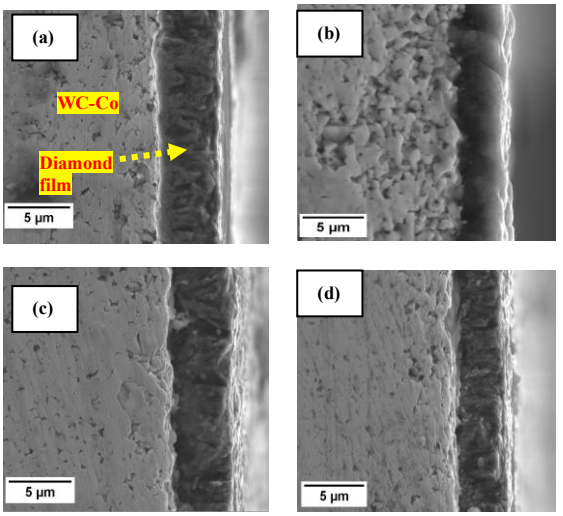

Fig.3. Cross section of WC-Co/Diamond film
a) MCD; b) NCD; c) BDD; d) BMTN

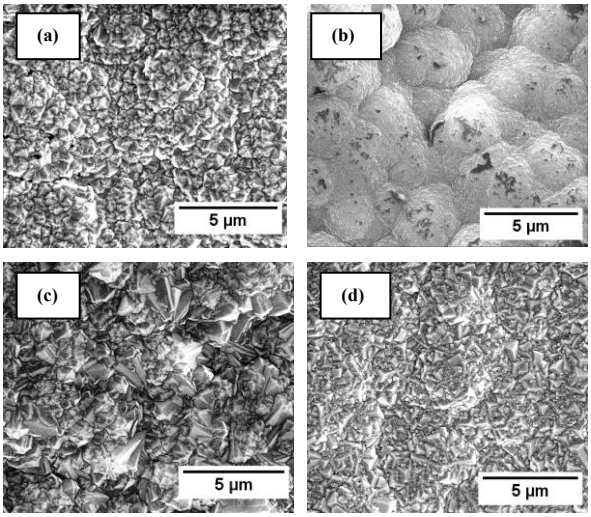

Fig.4. Surface morphology of distinct diamond coating variants
(a) MCD; (b) NCD; (c) BDD; (d) BMTN

3. Results and discussion

3.1 Surface morphology

The surface morphology of different diamond coating variants was observed using high-resolution scanning electron microscopy. Fig.4a shows the morphology of MCD coating. In MCD coating, the methane concentration is low, whereas process pressure is high, thus diamond grains begins to grow in a columnar fashion which leads to pyramidal shape structure in a range of ~ 0.75 – 1.5 µm. In contrast, for NCD coating, the re-nucleation of carbon atoms from methane occurs, thus grain size gets refining leads to ballas type structure with a grain size ~ 60-80 nm as shown in Fig.4b. With respect to BDD coating, the boron doping was introduced in MCD condition, hence yields similar pyramidal shape as shown in Fig.4c. However, the grain size gets increases from range ~ 1 – 1.5 µm due to defect induced boron clusters in the diamond lattice. In BMTN coating, the bottom layer was BDD coating followed by transition layer and top layer NCD coating. Transition layer will gradually transform the BDD coating to NCD coating. Thus the transition layer is usually a mix of these two coatings. Because of this phenomenon, the top layer ends with faceted structure with a grain size of ~ 300 – 500 nm as shown in Fig.4d.

3.2 Structural characterization

Raman spectroscopy is a non-destructive technique used to analyze the quality and phases of the diamond coating. Hence Raman analysis was considered for this present study to identify the distinct diamond coating variants.

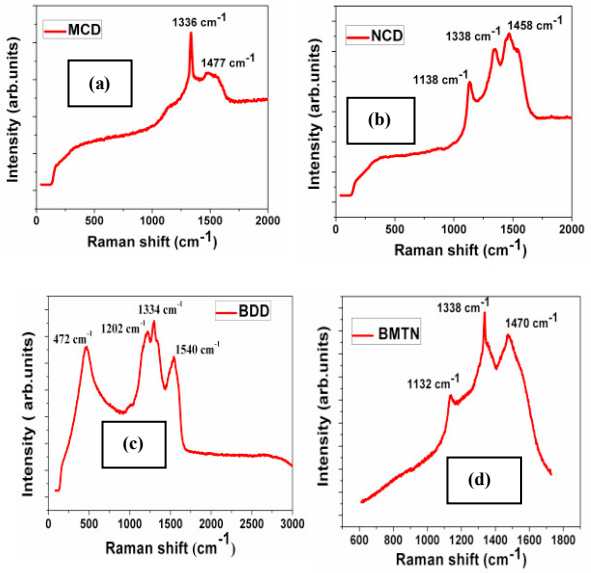

Fig.5. Raman spectrum of distinct diamond coating variants
(a) MCD; (b) NCD; (c) BDD; (d) BMTN

Fig.5a shows Raman spectra of MCD coating. Sharp Peak at 1336 cm^{-1} confirms the presence of

phase pure sp^3 diamond with a high degree of crystalline in the coating. On the other hand, for NCD coating, the broad peak at 1338 cm^{-1} along with trans-polyacetylene peaks at 1138 cm^{-1} confirms the signature of NCD as shown in Fig.5b. In addition, the high intensity of graphite peak at 1458 cm^{-1} confirms the typical sp^2 phase in the NCD coating as shown in Fig.5b. The peak at 472 cm^{-1} and 1202 cm^{-1} confirms the presence of B-B and B-C bonds along with a diamond peak at 1334 cm^{-1} confirms BDD coating as shown in Fig.5c. The peak at 1132 cm^{-1}, 1338 cm^{-1} confirms respective NCD layer in BMTN coating as shown in Fig.5d.

3.3 Surface Roughness

The surface roughness of the diamond coating was evaluated using contact type 2-D Perthometer. The total scanning length of 5.6 mm with cut off a length of 0.8 mm was taken to measure the surface roughness. Fig.6a shows surface variations recorded for MCD coating. Higher grain size with columnar growth on MCD coating leads to higher Ra value of 0.388 µm. The decrease in grain size with ballas type structure leads to lower Ra value of 0.066 µm as shown in Fig.6b for NCD coating. In BDD coating, the increase in grain size due to defect density contributes to the higher Ra value of 0.463 µm as shown in Fig.6c. For BMTN coating, the faceted structure due to gradual transformation in growth along with bottom layer BDD provides the Ra value of 0.269 µm as shown in Fig.6d.

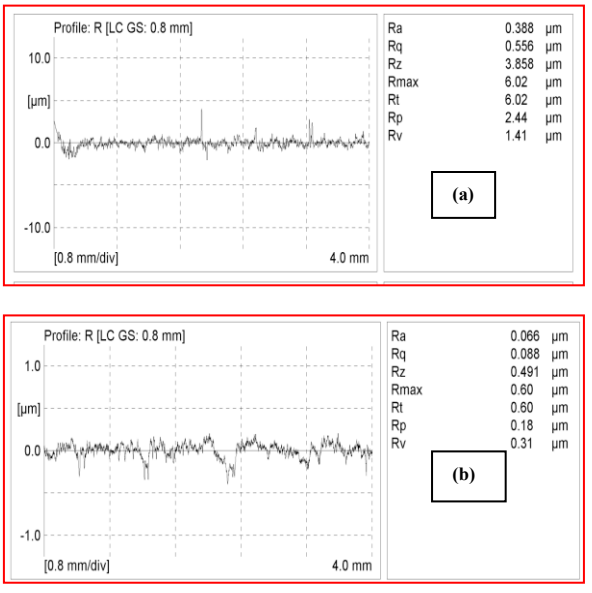

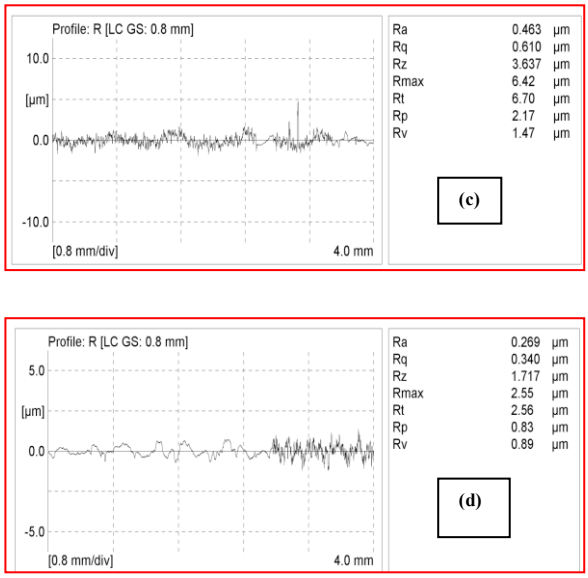

Fig.6. Surface roughness of distinct diamond coating variants (a) MCD; (b) NCD; (c) BDD; (d) BMTN

3.4 *Fracture toughness of the diamond film*

The Fracture toughness of the diamond film was calculated by using an Equ.1 [17] through Vicker's Indentation test method as shown in Fig.7 and measured toughness values were plotted as a bar graph shown in Fig.8. The Maximum Indentation load applied on the diamond film was 196 N. The hardness and Young's modulus of the diamond film were measured in one of our earlier paper [16].

$$K_{IC} = \alpha \left(\frac{E}{H} \right)^{\frac{1}{2}} \left(\frac{P}{C^{\frac{3}{2}}} \right) \quad (1)$$

K_{IC} = Fracture toughness of the film (MPa $m^{1/2}$)
α = 0.016 (Empirical constant)
E= Young's modulus of the film (MPa)
H = Hardness of the film (MPa)
P = Indentation load (N)
C= Radial crack length (µm)

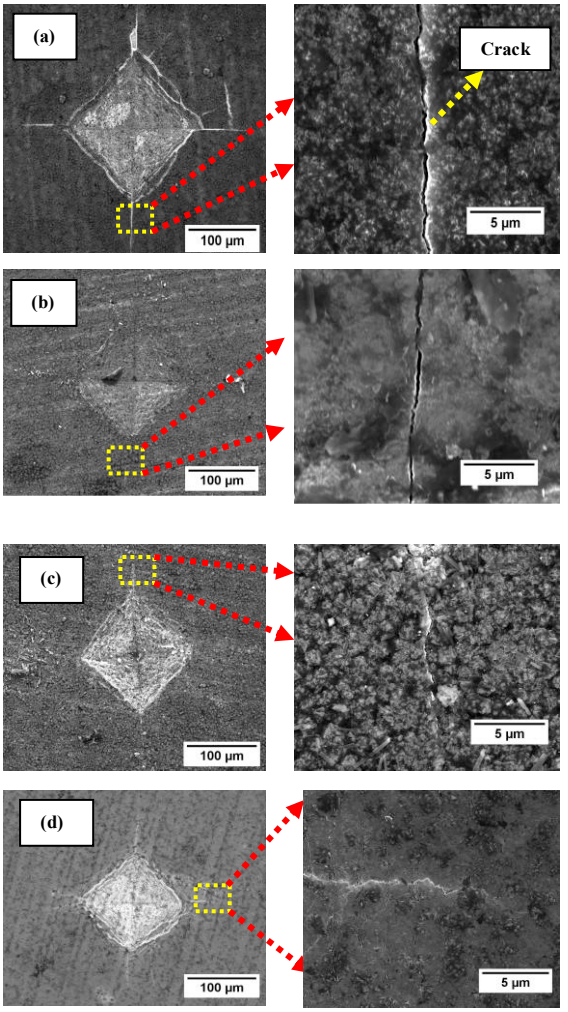

Fig.7. Vickers Indentation on the diamond film
(a) MCD; (b) NCD; (c) BDD; (d) BMTN

The measured crack length for MCD, NCD, BDD, and BMTN are found to be 159 µm, 183 µm, 124 µm and 109 µm respectively. The higher crack propagation for NCD attributes to the negative effects of sp^2 which causes poor coating adhesion. However less crack propagation for BDD and BMTN was due to the better coating adhesion through boron doping.

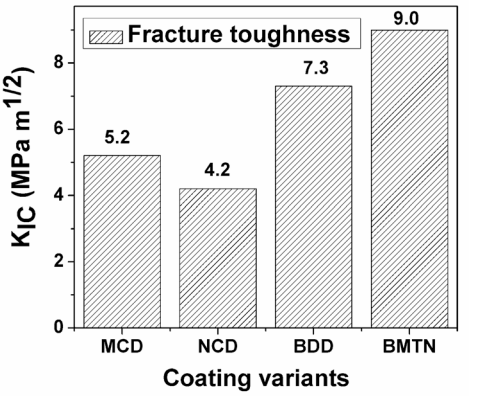

Fig.8. Fracture toughness graph for four coating variants

3.5 Work piece material and Machining

Aluminum-copper alloy (AA2124) with 25% reinforcement of silicon carbide particles (3-5µm) was considered as a work piece material as shown in Fig.9a. The uniform distributions of silicon carbide (SiC) particles in primary matrix aluminum-copper alloy were clearly seen in Fig.9a. The dimensions of workpiece material are 80 mm diameter and 300 mm length. The presence of two phases such as aluminum alloy and SiC can be easily distinguished from respective planes using X-ray diffraction analysis (XRD) as shown in Fig.9b.

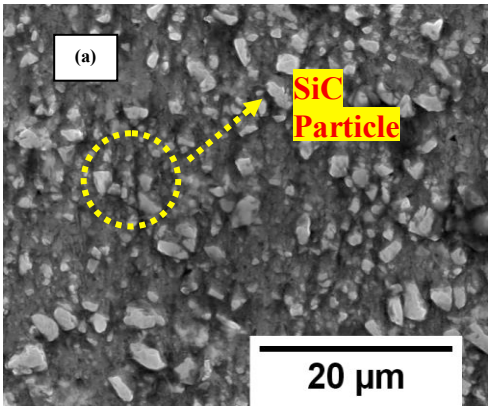

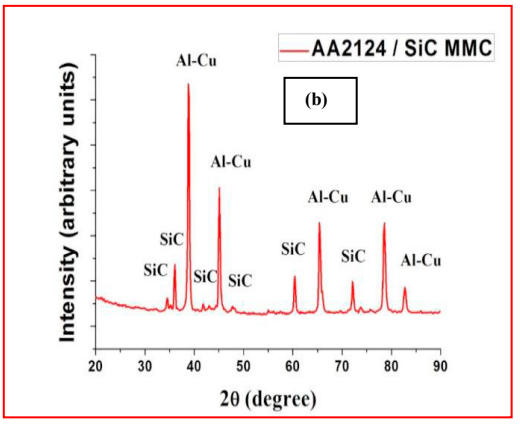

Fig.9. (a) SEM image of AA2124/25%SiCp
(b) XRD analysis on AA2124/25%SiCp

Machining experiment was conducted using VDF lathe (Heidenreich & Harbeck, Germany) has a maximum spindle speed of 5600 RPM, coupled with PIV drive attachment as shown in Fig.10. The Kistler piezoelectric 9257B dynamometer was attached to the tool holder to measure the corresponding cutting forces generated during machining. Tool wear experiment was conducted at a machining condition of 250 m/min cutting velocity, 0.05 mm/rev feed rate and 0.2 mm depth of cut respectively. The tool wear study was measured through a stereo microscope at an interval of 38 s each for a span of 160 mm machining length. The experiments were conducted three times and the corresponding flank wear with error value was shown in Fig.14. The overall machining length was 1120 mm and the corresponding time was calculated to be 4.4 minutes.

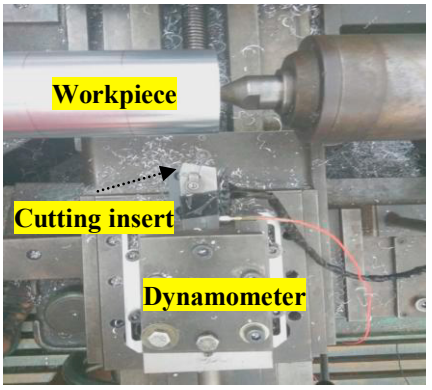

Fig.10. Machining set up

The maximum flank wear VB_{max} was limited to 0.2 mm for this present tool wear study.

3.6 Tool wear study

The wear performance of the distinct diamond coated tool was evaluated by using a tool wear experiment data. The final pass of the cutting force signals during tool wear study was illustrated in Fig.12. The tool cutting edge of the final cutting pass after machining was analyzed by scanning electron microscope (SEM). The SEM images of the cutting tool edge show adhesive and abrasive wear pattern during machining. Adhesive wear formation happens through built-up edge (BUE) formation, whereas abrasive wear occurs through SiC particle interaction with the tool. During machining of MMC, abrasive wear initiates first followed by aluminum BUE formation as a sticky on a worn area[18] as shown in Fig.11 in all cases. Fig.11 shows an SEM image of cutting tool after 1120 mm length machining. Fig.11a shows MCD tool after 1120 mm length machining. The measured flank wear VB_{max} = 0.23 mm for MCD coated tool, whereas VB_{max} = 0.28 for the NCD coated tool as shown in Fig.11b.

The Frictional force was calculated by using an Equ.2 for an oblique cutting [19] and the corresponding graph was shown in Fig.13.

$$F = P_n \times \sin\gamma_n + P_m \times \cos\gamma_n \quad (2)$$

$$P_m = F_X \times \sin\phi + F_Y \times \cos\phi \quad (3)$$

$$P_n = F_X \times \cos\phi \sin\lambda - F_Y \times \sin\phi \sin\lambda + F_Z \times \cos\lambda \quad (4)$$

Where F =Frictional force (N)
F_x = Feed force (N)
F_y = Radial force (N)
F_z = Thrust force (N)
γ_n = Normal Rake angle (º)
ϕ = Principal cutting edge angle (º)
λ = Inclination angle (º)

The measured forces in three axes such as F_x (Feed force), F_y (Radial force), F_z (Cutting force) are primarily responsible for the change in frictional force during machining. The higher frictional force promotes high wear on the tool cutting edges. With respect to MCD and NCD coating, the calculated frictional force forces was higher for NCD coating (23.14 N) than MCD coating (20.3 N) as shown in

Fig.13.This increase in frictional force in NCD coating could be due to the presence of sp^2 (non-diamond) phases in the coating. The presence of sp^2 phases negatively affects the interface adhesion of substrate-coating, which causes coating delamination. Thus NCD coating indicates high flank wear than MCD coating as shown in Fig.11b. In addition, the moderate fracture toughness of MCD (5.2 MPa $m^{1/2}$) poses mild edge chipping whereas very low fracture toughness of NCD (4.2 MPa $m^{1/2}$) shows high edge chipping as shown in Fig.11a,b. On the contrary for BDD (13.29 N) and BMTN cutting tool (8.99 N), the frictional force is relatively lower with MCD and NCD coating.

This results low flank wear in BDD (VB_{max} = 0.19 mm) and BMTN coating (VB_{max} = 0.18 mm). This enhanced wear resistance of BDD coating contributes to the lower frictional force and high fracture toughness (7.3 MPa $m^{1/2}$) which resists to edge chipping. The decrease in frictional force in BDD film attributed to the change in surface frictional energy through boron carbide chemical bonds exist in BDD film [20]. Perhaps cutting force signals indicates a gradual increase from 17 N to 21 N as shown in Fig.12c.

Eventually for BMTN coating, the measured flank wear relatively lower with BDD coating. This could be due to the very low frictional force combined with very high fracture toughness (9.0 MPa $m^{1/2}$). The corresponding cutting force signals generated a steady force of 24 N without any increase in force for BMTN as shown in Fig.12d.

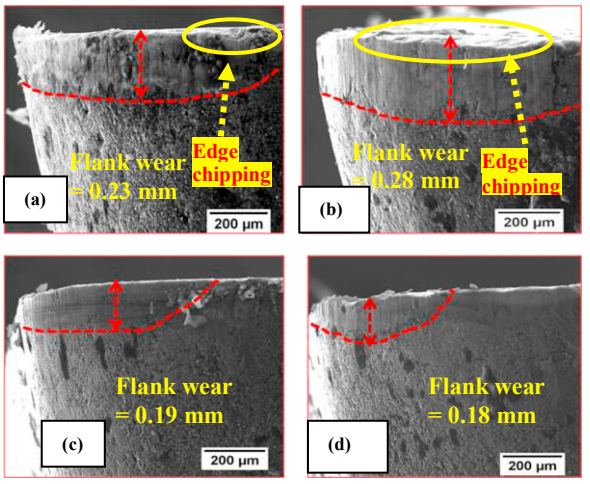

Fig.11. SEM image of cutting tool after 1120 mm length machining (a) MCD; (b) NCD; (c) BDD; (d) BMTN

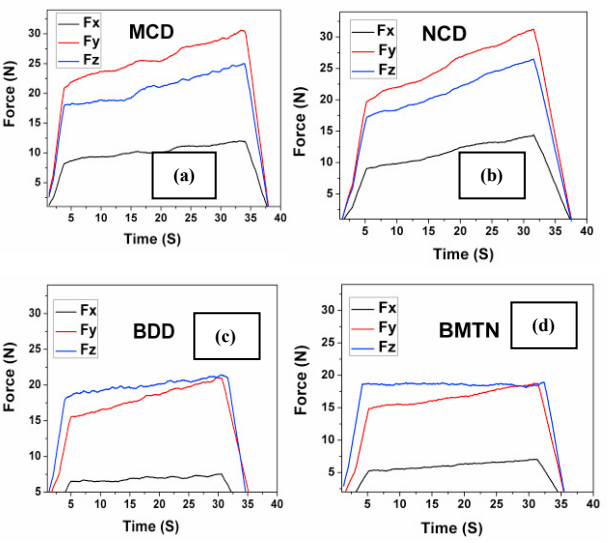

Fig.12. Cutting force graph of the final cutting pass (a) MCD; (b) NCD; (c) BDD; (d) BMTN

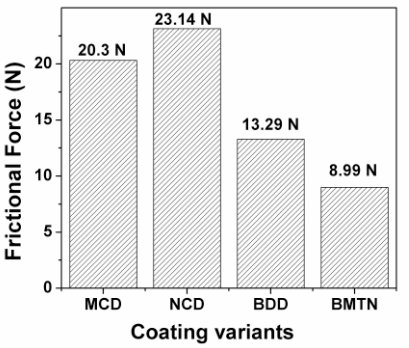

Fig.13. Frictional force graph for four coating variants

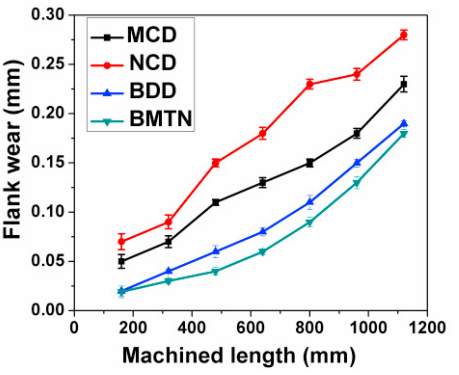

Fig.14. Machined length vs Flank wear

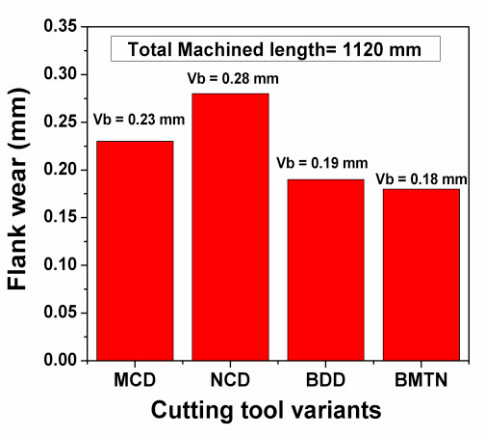

Fig.15. Cutting tool variants vs Flank wear

For a better understanding of complete tool wear study, the flank wear was plotted against the machining length of 1120 mm as shown in Fig.14. The wear at each distance can be observed with this tool wear plot. From Fig.15, the performance improvement of the MCD, NCD, and BDD coated cutting tools were compared with BMTN cutting tool by considering the values of respective flank wear.

BMTN = Flank wear = 0.18 mm
MCD = (0.23 – 0.18) ×100 = 21.7%
NCD = (0.28 – 0.18) ×100 = 35.7%
BDD = (0.19 – 0.18) ×100 = 5.2%

The calculated values show that boron-doped graded layer diamond coated tool (BMTN) was outperformed with MCD, NCD, and BDD with a percentage value of 21.7%, 35.7%, and 5.2% respectively.

4. Conclusions

The comparative performance of four distinct diamond coating variants such as MCD, NCD, BDD, and BMTN was discussed in detail through physical and mechanical characterization technique. The performance analysis of four coated tools was tested against machining of AA2124/25%SiC and the corresponding tool wear was discussed in this present study.

- The phases and quality of the diamond coatings were analyzed using Raman spectroscopy. Phase pure sp^3 for MCD and non- diamond phases of sp^2 in NCD and presence of boron signatures in BDD and BMTN were studied through this technique respectively.
- The surface roughness of the MCD, NCD, BDD, and BMTN coated WC-Co tools were correlated to the respective surface morphology of the coating.
- Fracture toughness of the coating were examined through Vicker's indentation test method. The results show that boron-doped graded layer diamond coating (BMTN) shows higher fracture toughness (9.0 MPa $m^{1/2}$) compared to other MCD, NCD and BDD coating.
- The tool wear study shows that MCD and NCD undergoes a Flank wear of VB_{max}= 0.23 mm and 0.28 mm whereas for BDD and BMTN coating shows a value of 0.19 mm and 0.18 mm respectively. The higher frictional force promotes high wear on the tool cutting edges. With respect to MCD and NCD coating, the calculated frictional forces show a value of 20.3 N and 23.14 N relatively higher compared to BDD (13.29 N) and BMTN coating (8.99 N). This results in low flank wear in BDD and BMTN coating. Thus, this study proves that boron-doped diamond coated cutting tools outperform with MCD, NCD and BDD coated tools during machining of AA2124/SiC_p MMC material.
- Thus boron doped graded layer diamond coated tool (BMTN) outperformed with MCD, NCD, and BDD with a percentage value of 21.7%, 35.7%, and 5.2% respectively.

Acknowledgements

MSR would like to thank funding from the Department of Science and Technology (DST), New Delhi that facilitated the creation of Nano Functional Materials Technology Centre (Grant: SR/NM/NAT-02/2005).

References

[1] N.P. Hung, C.H. Zhong, Cumulative tool wear in machining metal matrix composites Part I: Modelling, Journal of Materials Processing Technology, 58 (1996) 109-113.

[2] N. Tomac, K. Tannessen, F.O. Rasch, Machinability of Particulate Aluminium Matrix Composites, CIRP Annals, 41 (1992) 55-58.

[3] I. Ciftci, M. Turker, U. Seker, CBN cutting tool wear during machining of particulate reinforced MMCs, Wear, 257 (2004) 1041-1046.

[4] J.P. Davim, Diamond tool performance in machining metal–matrix composites, Journal of Materials Processing Technology, 128 (2002) 100-105.

[5] Y.K. Chou, J. Liu, CVD diamond tool performance in metal matrix composite machining, Surface and Coatings Technology, 200 (2005) 1872-1878.

[6] N. Muthukrishnan, M. Murugan, K. Prahlada Rao, Machinability issues in turning of Al-SiC (10p) metal matrix composites, The International Journal of Advanced Manufacturing Technology, 39 (2008) 211-218.

[7] S. Gururaja, M. Ramulu, W. Pedersen, Machining Of MMCs: A REVIEW, Machining Science and Technology, 17 (2013) 41-73.

[8] T.C.S. Vandevelde, K. Vandierendonck, M. Van Stappen, W. Du Mong, P. Perremans, Cutting applications of DLC, hard carbon and diamond films1Presented at the ICMCTF'98 Conference, San Diego, USA, April 1998.1, Surface and Coatings Technology, 113 (1999) 80-85.

[9] E. Uhlmann, J. Koenig, CVD diamond coatings on geometrically complex cutting tools, CIRP Annals, 58 (2009) 65-68.

[10] S.M. Alves, W. Albano, A.J. de Oliveira, Improvement of coating adhesion on cemented carbide tools by plasma etching, Journal of the Brazilian Society of Mechanical Sciences and Engineering, 39 (2017) 845-856.

[11] J.M. Arroyo, A.E. Diniz, M.S.F. de Lima, Cemented carbide surface modifications using laser treatment and its effects on hard coating adhesion, Surface and Coatings Technology, 204 (2010) 2410-2416.

[12] H. Gomez, D. Durham, X. Xiao, M. Lukitsch, P. Lu, K. Chou, A. Sachdev, A. Kumar, Adhesion analysis and dry machining performance of CVD diamond coatings deposited on surface modified WC–Co turning inserts, Journal of Materials Processing Technology, 212 (2012) 523-533.

[13] S. Balaji, M.S.R. Rao, C.R. Balkrishna, On the development of a dual-layered diamond-coated tool for the effective machining of titanium Ti-6Al-4V alloy, Journal of Physics D: Applied Physics, 50 (2017) 015302.

[14] X. Lei, L. Wang, B. Shen, F. Sun, Z. Zhang, Effect of Boron-Doped Diamond Interlayer on Cutting Performance of Diamond Coated Micro Drills for Graphite Machining, Materials, 6 (2013) 3128.

[15] X. Wang, Z. Lin, T. Zhang, B. Shen, F. Sun, Fabrication and application of boron-doped diamond coated rectangular-hole shaped drawing dies, International Journal of Refractory Metals and Hard Materials, 41 (2013) 422-431.

[16] K. Ramasubramanian, N. Arunachalam, M.S. Ramachandra Rao, Investigation on tribological behaviour of boron doped diamond coated cemented tungsten carbide for cutting tool applications, Surface and Coatings Technology, (2017).

[17] S. Zhang, X. Zhang, Toughness evaluation of hard coatings and thin films, Thin Solid Films, 520 (2012) 2375-2389.

[18] A. Kremer, A. Devillez, S. Dominiak, D. Dudzinski, M. El Mansori, Machinability Of Al/SiC Particulate Metal-Matrix Composites Under Dry Conditions With Cvd Diamond-Coated Carbide Tools, Machining Science and Technology, 12 (2008) 214-233.

[19] A.B.Chattopadhyay, Machining And Machine Tools Wiley, New Delhi, INDIA, 2011.

[20] L. Wang, X. Lei, B. Shen, F. Sun, Z. Zhang, Tribological properties and cutting performance of boron and silicon doped diamond films on Co-cemented tungsten carbide inserts, Diamond and Related Materials, 33 (2013) 54-62.